detritus | Multidisciplinary Journal for Circular Economy and Sustainable Management of Residues

CISA

MICROWAVE-BASED PYROMETALLURGICAL PROCESS TO PRODUCE FERROSILICON WITH PV CELLS FROM EOL PV PANELS

Emma Pitacco [1,*], Pietrogiovanni Cerchier [2], Mirko Pigato [1], Caterina Bernardini [3], Lorenzo D'Ambrosi [1], Michele Forzan [3] and Katya Brunelli [1]

[1] Department of Industrial Engineering, University of Padova, via Marzolo 9, 35131 Padova, Italy
[2] 9-Tech srl, Via Triestina bassa 74, 30020 Eraclea (VE), Italy
[3] Department of Industrial Engineering, University of Padova, via Gradenigo 6/A, 35131 Padova, Italy

Article Info:
Received:
12 June 2025
Revised:
25 August 2025
Accepted:
29 September 2025
Available online:
14 October 2025

Keywords:
Silicon
Waste
Microwave
Carbothermic
Ferrosilicon
Recycling

ABSTRACT

In this work, silicon recovered from a PV panel recycling facility was utilized as a reactant for the synthesis of ferrosilicon alloys via microwave treatment in the presence of iron oxides and graphite. Microwave-driven processing was further explored using ladle furnace slag from secondary steelmaking as a reactive component. Different amounts of reactants, time and microwave power were studied. Microwave heating allowed to reach temperatures higher than 900°C after few minutes of treatment at a power of 600 W. The materials were characterized by SEM-EDS and XRD. The proposed process allowed to obtain a ferrosilicon alloy with an amount of 21% Si. This study explored the use of three different types of waste, PV silicon, iron oxide and ladle furnace slag to obtain a ferroalloy FeSi which can be afterwards employed in the steelmaking process.

1. INTRODUCTION

In recent years, many significant advances were made regarding the recovery of silicon-based solid waste from the photovoltaic (PV) industry. In fact, the demand for silicon for PV production has increased due to the rise in raw materials cost, whereas the amount of global waste of PV panels is forecasted to reach 80 million tonnes by 2050 (Dubey et al., 2013; Guo et al., 2021; Preet & Smith, 2024): all these factors have stimulated the research in PV recycling.

Many studies demonstrated the feasibility of industrial-scale recovery of materials from end of life PV panels, showing that aluminium, silver, copper, glass, and silicon can be recovered (Cerchier et al., 2021; Huang et al., 2017; Pagnanelli et al., 2017). However, reintegration of the recovered silicon into the photovoltaic value chain still faces some challenges in terms of purity requirements and for now remains in the laboratory scale stage (Ngagoum Ndalloka et al., 2024). It is therefore essential to find new applications to extend the silicon reuse and promote sustainable waste recycling.

The possible routes to reclaim PV silicon waste are many, from processing it in order to meet the requirements of Si anodes for Li-ion batteries (C. Zhang et al., 2021), to using it as a leading element in the metallurgy of Si-based ferroalloys. Ferrosilicon plays a fundamental role in the deoxidizing and alloying of steel, their production being a very energy-intensive process.

A study proposed to synthesize ferrosilicon alloys by using waste glass and bakelite recovered from the automotive sector, showing an efficient reduction of iron oxide into Fe_3Si (gupeiite) (Farzana et al., 2014). Another work introduced a novel method for the production of ferrosilicon alloys, recovering two types of critical waste materials: Si PV cells and red mud. They demonstrated that the target composition of Fe-Si alloy could be achieved with Si deviations of 15 wt%, together with the formation of Fe-Si-Ti phases (Blaesing et al., 2024). The chemical composition of ferrosilicon alloys usually ranges between 15 and 90 wt% silicon, depending on the desired application. (Rauf Hurman, 2014).

The present study explores the possibility to employ different types of waste for producing ferrosilicon alloys, using microwave pyrometallurgical process to obtain a target composition respecting the ones typically found in the market; in particular, photovoltaic panels scrap and ladle furnace slag (LFS)as source of Si.

LFS (also known as "white" slag) is a by-product of ladle steelmaking refinement, characterized by a chemical composition rich in CaO, SiO_2, Al_2O_3, and MgO, along with oth-

* Corresponding author:
Emma Pitacco
email: emma.pitacco@studenti.unipd.it

https://doi.org/10.31025/2611-4135/2025.19538
© 2025 Cisa Publisher. All rights reserved

er trace elements (Najm et al., 2021). While it has chiefly been disposed of through landfilling, LFS has recently been recognized as a sustainable material for next generation eco-friendly construction industry (Aaros et al., s.d.; Yong et al., 2025; N. Zhang et al., 2025); its mineralogical properties make it in fact a suitable cement binder supplement or replacement (Adolfsson et al., 2011; Disconzi & Bellotto, 2025). These features further highlight its potential for integration into alternative recycling routes, such as the one presented in this study.

The proposed technique enables to perform a carbothermic reduction by using microwave radiation instead of conventional furnace treatments, therefore not only promoting an opened-loop recycling path for PV-Si and LFS, but also testing the efficiency of alternative and more eco-friendly energy sources.

The use of microwaves to perform reduction reactions of different types of ores has recently gained a lot of attention, owing to its good heat selectivity and rapid processing times (Peng & Hwang, 2015). For instance, studies conducted on MW-processed low-grade iron ores demonstrated that reduction was achieved in 10 minutes, reaching temperatures in the order of 800°C (Rayapudi et al., 2020).

In this study a characterization of the products obtained from MW heating was carried out, evaluating the feasibility of achieving a carbothermic reduction of iron ores mixed with Si-based PV cells, recovered from waste PV panels, and ladle furnace slag, another waste produced by the steelmaking industry.

2. MATERIALS AND METHODS

2.1 Materials

Recycled silicon wafer fragments for the experiments performed in this study were supplied by 9-Tech (Venice, Italy), from their pilot plant in Venice. In this facility, raw materials from photovoltaic panels are recovered through a thermomechanical treatment, which enables the separation of glass, aluminium, copper, and PV cell fragments. The latter can be further processed using ultrasound treatment to remove silver and aluminum. After this step, the fragments consist mainly of metallic silicon (>96%) and aluminum (<3%). (Cerchier et al., 2024). The treated PV cells were ground with a ball milling machine operated at 30 Hz for 10 s, until a particle size below 45 μm was obtained.

The iron oxides mix and ladle furnace slag used for conducting the experiments were supplied by a company in Northern Italy.

Synthetic graphite (<20 μm, SigmaAldrich) was added to the powder mix as a reducing reagent as well as heating element, owing to its high absorbance ability towards microwaves.

Before microwave heat treatment, the powders were dried for 24 hours in a BINDER FD 53 heating chamber.

2.2 Experimental

A domestic Panasonic NN-GD351W microwave oven operating at 2.45 GHz frequency was used for pyrometallurgical tests, which were performed in air atmosphere.

Alumina crucibles were used as powder containers for the reaction and a silicon carbide (SiC) susceptor was employed as a heating auxiliary. In fact, dielectric materials like SiC strongly absorb microwave radiation and can therefore passively help the heating of a reaction mixture in the MW field by converting electromagnetic energy into thermal energy (Ishizaki & Nagata, 2007; Singh et al., 2024).

The temperature of the specimens during the experiments was measured by means of a FLIR T420 infrared camera.

The weight in grams (g) of each reactant used in the experiments is reported in Table 1, while the selected process parameters are reported in Table 2 .

The input reagents underwent crystallographic analysis through X-ray diffraction (Bruker D8 Advance, Karlsruhe, Germany), conducted in the 2θ range of 15-75°, with a step size of 0.02° and a counting time of 1 s. The X-ray diffraction spectra of all the input reagents are presented in Figure 1.

Sample 1 was obtained by mixing equal fractions of slag and metallic PV-Si, which was distributed at the bottom of the crucible to create a powder bed. The sample was treated at 600 W for 70 s.

Test 2 was performed maintaining the powder proportions of test 1 but decreasing the overall weight to 0.37 g. The experiment was carried out at 600 W for 120 s.

A third experiment was carried out with the same process parameters of test 2 on a sample with equal amounts

TABLE 1: Weight (g) of the reactants used for each experiment.

Sample	Iron oxide [g]	White slag [g]	PV Si [g]	Graphite [g]
1	0.304	0.117	0.106	0.202
2	0.153	0.053	0.055	0.105
3	0.1	-	0.1	0.1

TABLE 2: Microwave process parameters for each test.

Sample	Power [W]	Time [s]	Susceptor	Total weight [g]
1	600	70	No	0.7
2	600	120	Yes	0.37
3	600	120	Yes	0.3

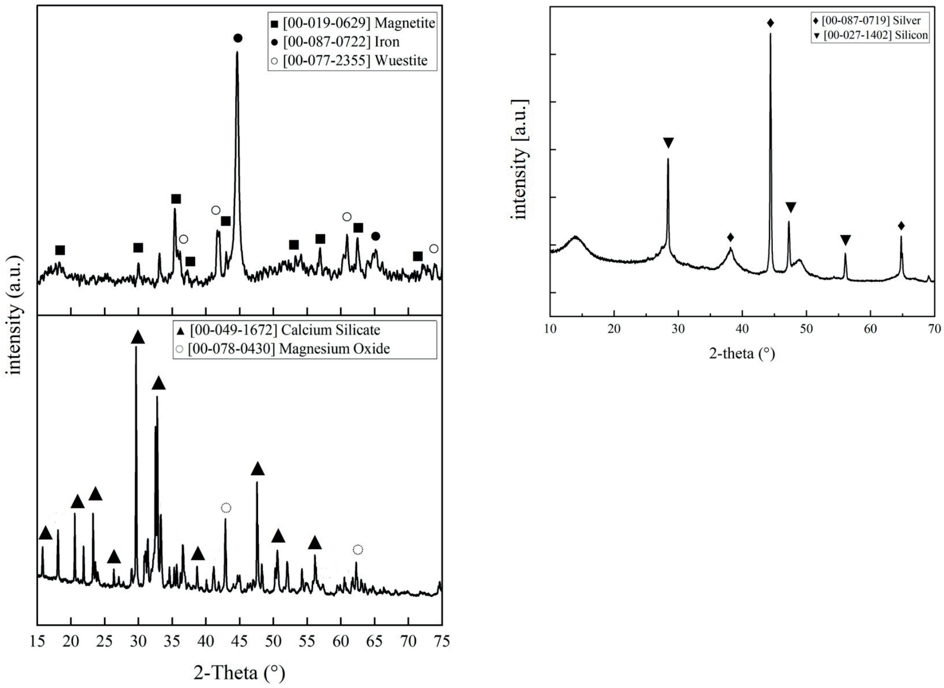

FIGURE 1: a-c) XRD spectra of the input reagents.

of iron oxide, PV-Si and graphite, without adding the white slag powder.

The MW treated metallic samples were mounted into a polymeric resin and polished with standard metallographic preparation as per ASTM E3.

A Zeiss EVO-M10 scanning electron microscope (SEM), equipped with an Oxford Instruments energy-dispersive X-ray spectroscopy (EDS) detector was employed for surface characterization of the specimens.

3. RESULTS AND DISCUSSION

3.1 Results

The specimens obtained after microwave heating were cooled in air and then carefully examined in order to identify the formation of alloys from the initial powder. During microwave exposure of the samples, the reactants are heated with the aid of the susceptor, until they reach a high enough temperature to react with each other and melt. During the reaction, oxidation of the graphite into CO_2 takes place, while iron oxides are reduced into metallic iron. When MW irradiation is interrupted, the molten material starts solidifying and during its cooling off, alloy particles are formed until room temperature is reached.

From SEM characterization images in back scattered electrons mode (BSE) it was observed that the alloy nuggets often nucleated from white slag particle clusters, as inferred from the EDS spectrum 1 in Figure 2, showing peaks belonging to Ca, Si, Al and Mg oxides. Given the higher atomic weight of iron, the alloy colour appears white compared to the slag, which instead appears gray/black.

From low magnification SEM analysis of the particles of sample 1, the majority of the metallic areas seems to be made of iron and carbon nodules, forming a structure similar to that of nodular cast iron (Figure 3).

However, at higher magnification the presence of small biphasic regions rich in both Fe and Si was detected (Figure 4).

Composition analysis performed with EDS demonstrated that the darker phase is characterized by a higher silicon content, while the lighter is enriched in manganese, as can be observed in the elemental map of Figure 5. The ratio between Si and Fe is equal to about 3:1 (Table 3).

Specimen 2 was subjected to a weight loss of 16% after microwave treatment, probably caused by the formation of CO and CO_2 gases produced by the carbothermic reaction. Thermal camera pictures were taken after 30, 60 and 100 s during the experiment (Figure 6) and display a significant increase in the temperature after 1 minute of exposure to microwaves, reaching a maximum of 930°C at the end of the test.

EDS analysis (Figure 7) shows that the selected test parameters allowed to obtain alloy particles with varying contents of Si, while oxygen and other elements were undetected. Magnification of such areas confirmed the formation of the two different phases: the lighter one containing about 16 wt % Si and 1.13 wt % Mn, respectively, while the darker one 23 wt % Si and 2.27 wt % Mn. The bright white particles were instead found to be impurities of Sn and Cu, probably belonging to some residues from the welded joints in PV electronic circuits.

The third sample was obtained without adding the LFS fraction, to verify how its presence affected the composition of the alloy. SEM analysis showed a morphology very similar to the one observed in cast iron, with carbon floccules dispersed in a Fe matrix (Figure 8). EDS analysis outlined a content of Si equal to 16 wt %.

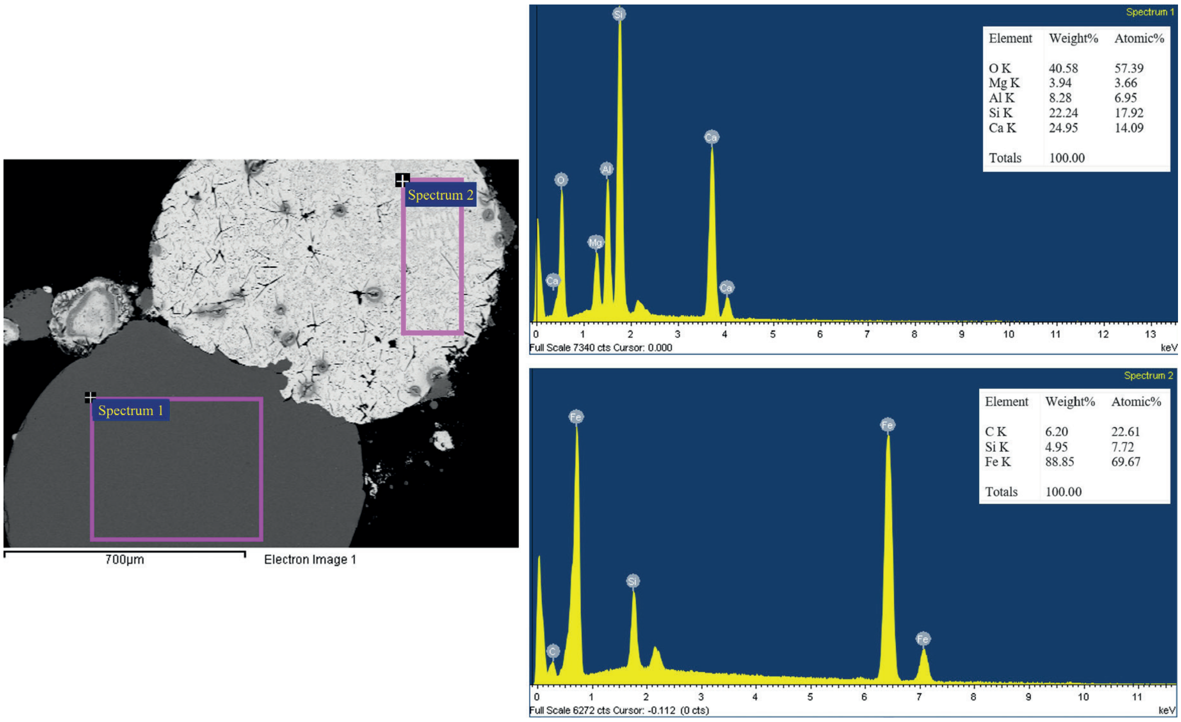

FIGURE 2: SEM-BSE and EDS spectrum of alloy nugget nucleated from LFS granule (sample 1).

3.2 Discussion

Characterization of the MW-synthesized samples demonstrates the feasibility of producing a silicon ferroalloy with MW treatment of silicon PV cells and LFS in presence of iron oxides and graphite.

For sample 1, the addition of a limited amount of Si PV cells powder allowed to obtain the localized formation of a FeSi alloy, unevenly distributed throughout the LFS matrix. The EDS spectrum denoted a content of silicon lower than 10%, which is slightly below the required levels for the pro-

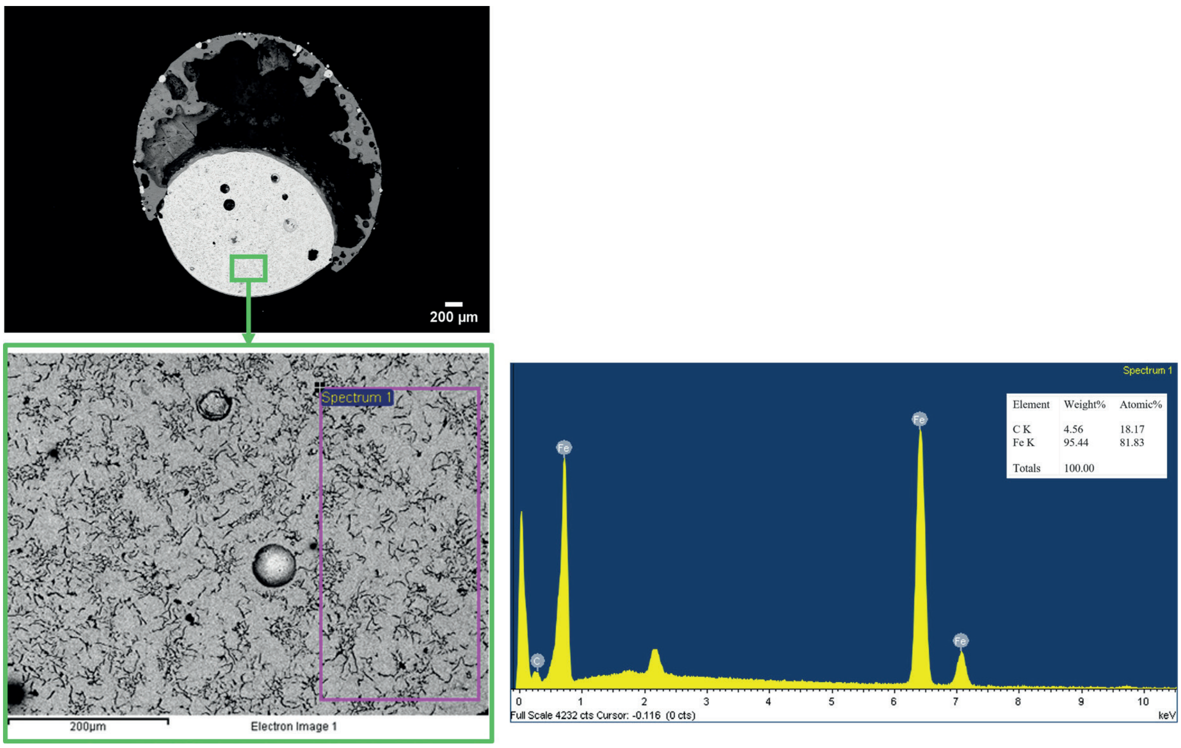

FIGURE 3: SEM-EDS of metallic area in sample 1.

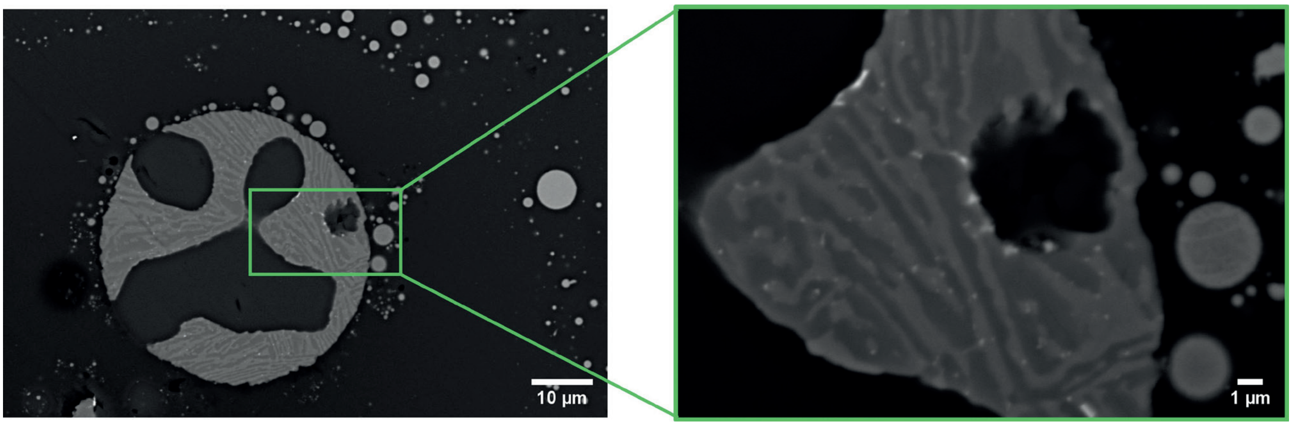

FIGURE 4: High SEM-BSE magnification of biphasic FeSi alloy detected in sample 1.

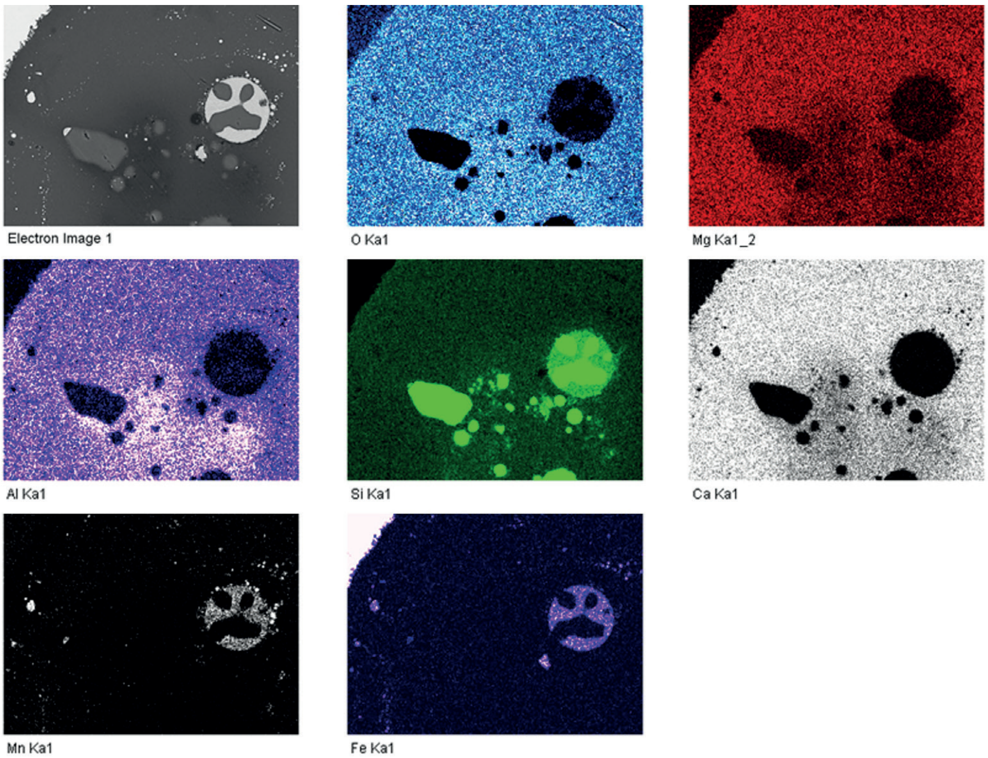

FIGURE 5: SEM-EDS elemental map of FeSi alloy in sample 1.

duction of ferrosilicon (Rauf Hurman, 2014). The majority of metallic particles synthesized during the treatment exhibited a composition rich in iron and carbon, without a discernible presence of silicon. The low content of silicon in the alloy of sample 1 is likely due to low reaction efficiency, possibly resulting from the absence of the SiC susceptor and thus the inability to reach the required temperature for suitable element diffusion.

Experiment 2 led to the formation of a FeSi alloy in which the composition of 15-23 wt% silicon is consistent with the lower limit of the ranges usually required for ferrosilicon alloys.

The lower total weight of the reactants of test 2 (0.37 g) compared to test 1 (0.73 g) probably supported a more effective utilization of the output electromagnetic energy, facilitating the efficient volumetric heating of a smaller

TABLE 3: Chemical composition of Fe-Si-Mn alloy particle formed during test 1.

Elements [wt. %]	Si	Cr	Mn	Fe	Ti
Dark phase	67.98	0.72	10.18	21.11	-
Light phase	61.52	2.14	20.05	14.85	1.44

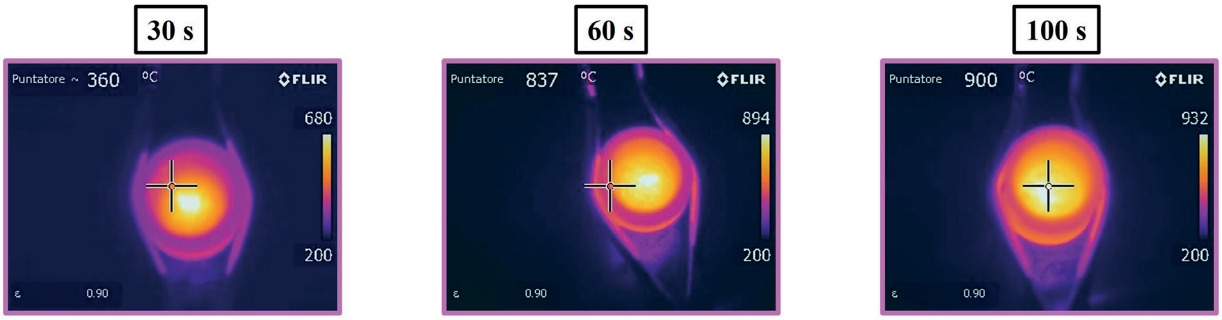

FIGURE 6: Thermal camera images taken during test 2.

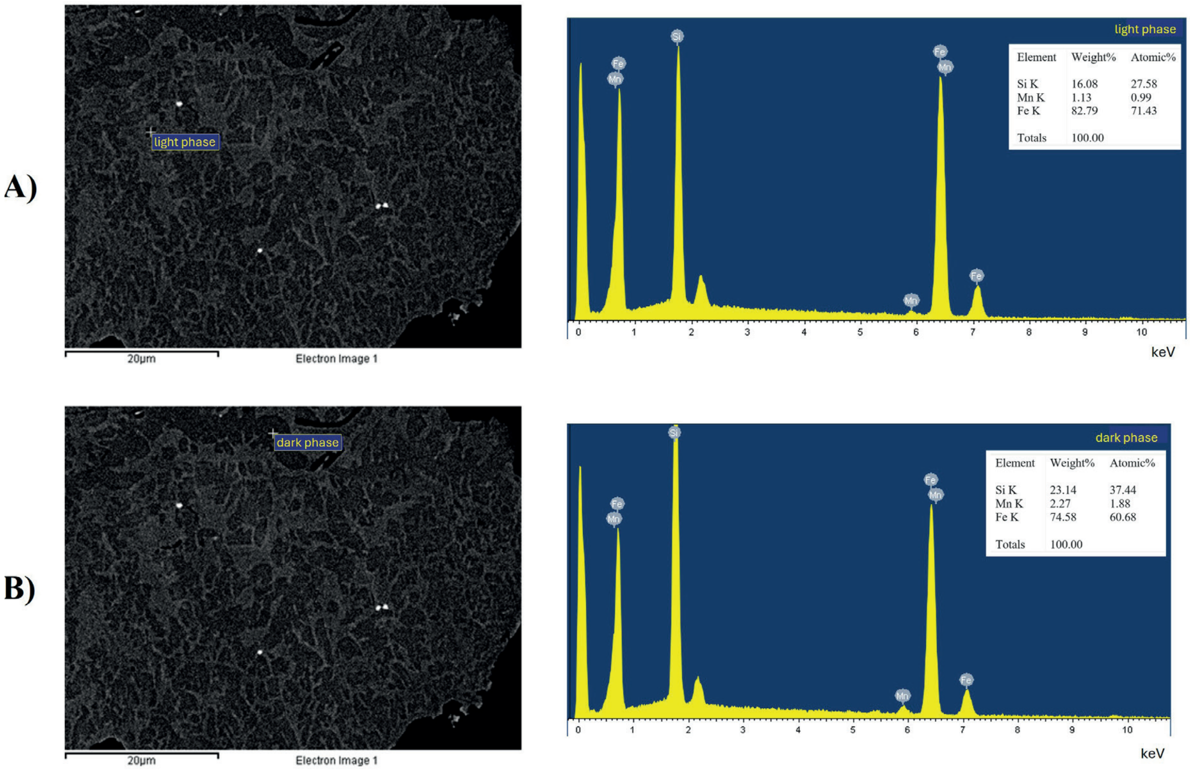

FIGURE 7: EDS spectra of the two phases detected in specimen 2.

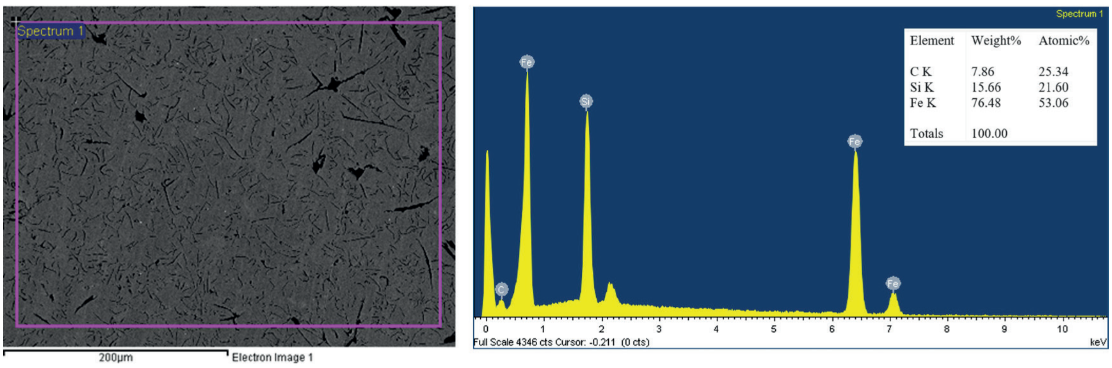

FIGURE 8: EDS spectrum of alloy in sample 3.

amount of powder. An approximate estimate of the energy consumed to heat sample 2 can be obtained by considering that by setting a power of 600 W and heating for 120 s, the required theoretical energy would be of 72 kJ (energy = power * time). Other more detailed studies on the efficiency of MW heating assert that its energy consumption can be a hundred times lower than the one of, for example, electrical heating (Zhu et al., 2018).

Moreover, presence of the SiC susceptor and setting of longer microwave exposure time contributed to a more resource-effective carbothermic reaction.

Compared to test 2, test 3 (during which LFS was not added to the reaction) led to the formation of a ferrosilicon alloy with lower silicon content (about 16 wt%). However, the reaction outcome seems to be promising and could be further optimized.

4. CONCLUSIONS

The present study has demonstrated that it is possible to produce a Si ferroalloy using a microwave pyrometallurgical process, which utilizes silicon recovered from PV panels, white slag, and iron oxides as reagents, and graphite as a reducing agent. The performed experiments showed that all the reactant dosages led to the synthesis of a ferrosilicon alloy, differing in the composition due to different reaction efficiencies. SEM-EDS characterization of the specimens highlighted that the alloy reached the target composition by adding equal proportions of PV-Si and LFS. This result was obtained after optimization of the total weight of the specimen and of the MW parameters, leading to the conclusion that longer exposure time for a smaller amount of powder facilitated the carbothermic reaction.

Thermal camera images revealed that the required temperatures for the pyrometallurgical process can be reached after only 100 s of MW exposure.

In the future, further research will be carried out for larger-scale production of ferrosilicon by microwave heating.

ACKNOWLEDGEMENTS

This research was supported by Department of Industrial Engineering, University of Padua (BIRD 2023 project) and by EIT Raw Materials (PARSIVALPLUS project).

REFERENCES

Aaros, P., Aponte, D., Lavin, R., & Barra, M. (s.d.). Sustainable Portland Cement Alternative: Alkaline Activation of Ladle Furnace Slag as a Precursor for Eco-Friendly Building Materials. Journal of Materials in Civil Engineering, 37(5). https://doi.org/10.1061/JMCEE7.MTENG-18856

Adolfsson, D., Engström, F., Robinson, R., & Björkman, B. (2011). Cementitious Phases in Ladle Slag. Steel Research International, 82(4), 398–403. https://doi.org/10.1002/srin.201000176

Blaesing, L., Walnsch, A., Hippmann, S., Modrzynski, C., Weidlich, C., Pavón, S., & Bertau, M. (2024). Ferrosilicon Production from Silicon Wafer Breakage and Red Mud. ACS Sustainable Resource Management, 1(3), 404–416. https://doi.org/10.1021/acssusresmgt.3c00035

Cerchier, P., Brunelli, K., Pezzato, L., Audoin, C., Rakotoniaina, J. P., Sessa, T., Tammaro, M., Sabia, G., Attanasio, A., Forte, C., Nisi, A., Suitner, H., & Dabalà, M. (2021). Innovative recycling of end of life silicon PV panels: ReSiELP. Detritus, 41–47. https://doi.org/10.31025/2611-4135/2021.15118

Cerchier, P., Miserocchi, F., Pezzato, L., Nisato, F., Tassinato, G., Grigolato, C., Dabalà, M., & Brunelli, K. (2024). Photovoltaic panel recycling: Tests in the pilot plant in Venice and silicon applications for ferroalloy production. Detritus, 29, 54–62. https://doi.org/10.31025/2611-4135/2024.19436

Disconzi, F., & Bellotto, M. (2025). Production of Synthetic Hydraulic Binder Precursors from Steel Slags: Experimental Validation and Thermodynamic Simulation. Proceedings of the RILEM Spring Convention and Conference 2024, 208–215. https://doi.org/10.1007/978-3-031-70277-8_24

Dubey, S., Jadhav, N. Y., & Zakirova, B. (2013). Socio-Economic and Environmental Impacts of Silicon Based Photovoltaic (PV) Technologies. Energy Procedia, 33, 322–334. https://doi.org/10.1016/j.egypro.2013.05.073

Farzana, R., Rajarao, R., & Sahajwalla, V. (2014). Synthesis of ferrosilicon alloy using waste glass and plastic. Materials Letters, 116, 101–103. https://doi.org/10.1016/j.matlet.2013.10.105

Guo, J., Liu, X., Yu, J., Xu, C., Wu, Y., Pan, D., & Senthil, R. A. (2021). An overview of the comprehensive utilization of silicon-based solid waste related to PV industry. Resources, Conservation and Recycling, 169, 105450. https://doi.org/10.1016/j.resconrec.2021.105450

Huang, W.-H., Shin, W. J., Wang, L., Sun, W.-C., & Tao, M. (2017). Strategy and technology to recycle wafer-silicon solar modules. Solar Energy, 144, 22–31. https://doi.org/10.1016/j.solener.2017.01.001

Ishizaki, K., & Nagata, K. (2007). Selectivity of Microwave Energy Consumption in the Reduction of Fe3O4 with Carbon Black in Mixed Powder. Isij International - ISIJ INT, 47, 811–816. https://doi.org/10.2355/isijinternational.47.811

Najm, O., El-Hassan, H., & El-Dieb, A. (2021). Ladle slag characteristics and use in mortar and concrete: A comprehensive review. Journal of Cleaner Production, 288, 125584. https://doi.org/10.1016/j.jclepro.2020.125584

Ngagoum Ndalloka, Z., Vijayakumar Nair, H., Alpert, S., & Schmid, C. (2024). Solar photovoltaic recycling strategies. Solar Energy, 270, 112379. https://doi.org/10.1016/j.solener.2024.112379

Pagnanelli, F., Moscardini, E., Granata, G., Abo Atia, T., Altimari, P., Havlik, T., & Toro, L. (2017). Physical and chemical treatment of end of life panels: An integrated automatic approach viable for different photovoltaic technologies. Waste Management, 59, 422–431. https://doi.org/10.1016/j.wasman.2016.11.011

Peng, Z., & Hwang, J.-Y. (2015). Microwave-assisted metallurgy. International Materials Reviews, 60(1). https://doi.org/10.1179/1743280414Y.0000000042

Preet, S., & Smith, S. T. (2024). A comprehensive review on the recycling technology of silicon based photovoltaic solar panels: Challenges and future outlook. Journal of Cleaner Production, 448, 141661. https://doi.org/10.1016/j.jclepro.2024.141661

Rauf Hurman, E. (2014). Production of Ferroalloys. In S. Seetharaman (A c. Di), Treatise on Process Metallurgy (pp. 477–532). Elsevier. https://doi.org/10.1016/B978-0-08-096988-6.00005-5

Rayapudi, V., Agrawal, S., & Dhawan, N. (2020). Evaluation of carbothermal reduction for processing of banded hematite jasper ore. Powder Technology, 362, 826–834. https://doi.org/10.1016/j.powtec.2019.09.094

Singh, S., Bhaskar, R., Narayanan, K. B., Kumar, A., & Debnath, K. (2024). Development of silicon carbide (SiC)-based composites as microwave-absorbing materials (MAMs): A review. Journal of the European Ceramic Society, 44(13), 7411–7431. https://doi.org/10.1016/j.jeurceramsoc.2024.05.032

Yong, C. L., Tan, T. H., Ghayeb, H. H., Koting, S., & Mo, K. H. (2025). Role of sulphate-based additives on the early age properties of Portland cement incorporating alumina-rich ladle furnace slag. Case Studies in Construction Materials, 22, e04336. https://doi.org/10.1016/j.cscm.2025.e04336

Zhang, C., Ma, Q., Cai, M., Zhao, Z., Xie, H., Ning, Z., Wang, D., & Yin, H. (2021). Recovery of porous silicon from waste crystalline silicon solar panels for high-performance lithium-ion battery anodes. Waste Management, 135, 182–189. https://doi.org/10.1016/j.wasman.2021.08.037

Zhang, N., Deng, G., Liao, W., Hu, C., & Ma, H. (2025). Positive effects of sulfates on performance of cement paste incorporating low-grade, high-aluminum steel slag. Cement and Concrete Composites, 162, 106134. https://doi.org/10.1016/j.cemconcomp.2025.106134

Zhu, J., Yang, Z., Li, X., Qi, S., & Jia, M. (2018). Application of microwave heating with iron oxide nanoparticles in the in-situ exploitation of oil shale. Energy Science & Engineering, 6(5), 548–562. https://doi.org/10.1002/ese3.231